Plant cover as an estimator of above-ground biomass in semi-arid woody vegetation in Northeast Patagonia, Argentina

Laura B RODRIGUEZ[1,2], Silvia S TORRES ROBLES[1*], Marcelo F ARTURI[3], Juan M ZEBERIO[1], Andrés C H GRAND[4], Néstor I GASPARRI[5,6]

[1] National University of Río Negro, Atlantic Headquarters, Center for Environmental Studies from Norpatagonia (CEANPa), Viedma 8500, Argentina;
[2] National Council of Scientific and Technical Research (CONICET), Viedma 8500, Argentina;
[3] Ecological and Environmental Systems Research Laboratory (LISEA), National University of La Plata, La Plata 1900, Argentina;
[4] National Institute of Agricultural Technology (INTA), AER Patagones, Carmen de Patagones 8504, Argentina;
[5] Institute of Regional Ecology (IER), National University of Tucumán (UNT)-National Council of Scientific and Technical Research (CONICET), Tucumán 4000, Argentina;
[6] Faculty of Natural Sciences and Miguel Lillo Institute, National University of Tucumán (UNT), Yerba Buena 4107, Argentina

Abstract: The quantification of carbon storage in vegetation biomass is a crucial factor in the estimation and mitigation of CO_2 emissions. Globally, arid and semi-arid regions are considered an important carbon sink. However, they have received limited attention and, therefore, it should be a priority to develop tools to quantify biomass at the local and regional scales. Individual plant variables, such as stem diameter and crown area, were reported to be good predictors of individual plant weight. Stand-level variables, such as plant cover and mean height, are also easy-to-measure estimators of above-ground biomass (AGB) in dry regions. In this study, we estimated the AGB in semi-arid woody vegetation in Northeast Patagonia, Argentina. We evaluated whether the AGB at the stand level can be estimated based on plant cover and to what extent the estimation accuracy can be improved by the inclusion of other field-measured structure variables. We also evaluated whether remote sensing technologies can be used to reliably estimate and map the regional mean biomass. For this purpose, we analyzed the relationships between field-measured woody vegetation structure variables and AGB as well as LANDSAT TM-derived variables. We obtained a model-based ratio estimate of regional mean AGB and its standard error. Total plant cover allowed us to obtain a reliable estimation of local AGB, and no better fit was attained by the inclusion of other structure variables. The stand-level plant cover ranged between 18.7% and 95.2% and AGB between about 2.0 and 70.8 Mg/hm^2. AGB based on total plant cover was well estimated from LANDSAT TM bands 2 and 3, which facilitated a model-based ratio estimate of the regional mean AGB (approximately 12.0 Mg/hm^2) and its sampling error (about 30.0%). The mean AGB of woody vegetation can greatly contribute to carbon storage in semi-arid lands. Thus, plant cover estimation by remote sensing images could be used to obtain regional estimates and map biomass, as well as to assess and monitor the impact of land-use change on the carbon balance, for arid and semi-arid regions.

Keywords: above-ground biomass; shrublands; ratio estimation; carbon storage; remote sensing; Patagonia

Corresponding author: Silvia S TORRES ROBLES (storresr@unrn.edu.ar)
Received 2021-04-07; revised 2021-07-30; accepted 2021-08-09

1 Introduction

The loss of biomass is an important cause of increased greenhouse emissions mainly promoted by land-use change (Foley et al., 2005; Houghton, 2005). Thus, a decrease in deforestation rates is considered an important strategy to reduce CO_2 emissions (Kindermann et al., 2008). In this context, carbon storage in vegetation biomass represents a valuable environmental service, and its quantification is, therefore, an important measurement to estimate and mitigate CO_2 emissions from deforestation (Houghton, 2007; GTOS, 2010). Carbon storage has been widely studied, especially in tropical and subtropical forests, over the last decades (Baccini et al., 2008; Saatchi et al., 2011; Gasparri et al., 2013; Hansen et al., 2013; Cartus et al., 2014; Hengeveld et al., 2015). However, the carbon storage of woody communities in arid and semi-arid regions has received much less attention (Grainger, 1999; Malagnoux et al., 2007; Le Polain de Waroux and Lambin, 2012). Globally, arid and semi-arid regions are considered an important carbon sink since they cover approximately 45.0% of the land area of the world (Grünzweig et al., 2003; Nosetto et al., 2006).

In dry ecosystems, tree cover and shrub cover are closely related to carbon storage, and their spatio-temporal features are strongly dependent on climate, soil, herbivory, wildfire frequency, and land-use change (Sankarán et al., 2005; Torres Robles et al., 2015; Zeberio and Pérez, 2020). Field estimation of biomass vegetation in arid and semi-arid regions is usually more difficult than it is in temperate forest regions due to the lack of classical tools such as national forest inventories and the standardized biomass equations available for trees (Le Polain de Waroux and Lambin, 2012). Therefore, it is a priority to develop tools to quantify biomass at the local and regional scales, to correctly estimate the impact of land-use change on the carbon balance of these arid and semi-arid ecosystems.

At the local scale, above-ground biomass (AGB) is frequently estimated through dimensional analysis, based on the allometric relationship between the plant dimension and the dry mass for individual species or species groups (Jenkins et al., 2004). Stem base diameter and diameter at breast height (DBH) are the most common and useful variables to estimate biomass at the individual tree level (Chave et al., 2005; Fonseca et al., 2009). In multi-stemmed woody species, the most useful variables are those related to the crown size because this is the best way to represent the plant volume (Hierro et al., 2000; Hofstad, 2005; Oñatibia et al., 2010; Conti et al., 2019). However, allometric formulas for the estimation of tree and shrub biomass are not always available, especially for semi-arid vegetation, which is usually dominated by small trees and multi-stemmed shrubs (Hierro et al., 2000; Conti et al., 2013). In addition, serious difficulties arise when allometric models are used in the field because time-demanding variables must be measured. Furthermore, individuals are not isolated; instead, overlapping crowns are frequently found among individuals of the same or different species (Torres Robles et al., 2015; Zeberio et al., 2018). Alternatively, stand-level vegetation variables, such as plant cover and mean height, were shown to be easy-to-measure independent variables to estimate AGB in dry regions (Flombaum and Sala, 2007; Chojnacky and Milton, 2008; Pearce et al., 2010). Moreover, plant cover has been highlighted as a good single variable estimator of vegetation biomass in arid or semi-arid shrublands (Flombaum and Sala, 2007; Zhang et al., 2019), which can be appropriately estimated from remote sensing images.

At the regional scale, remote sensing techniques have been considered valid tools for mapping and monitoring forest biomass (Dong et al., 2003; Houghton, 2005; Dengsheng, 2006). Statistical approaches are commonly used to link field data with remote sensing information in arid and semi-arid regions (Dengsheng, 2006; Chen et al., 2010). These approaches seek relationships between the vegetation biomass measured in the field and spectral variables (Galidaki et al., 2017; Chen et al., 2018). However, models to estimate AGB derived from remote sensing images are

specific for a given region at a given moment and have low transferability in space and time (Eisfelder et al., 2012). Thus, local and regional estimates of AGB are needed to understand the dynamics of carbon storage in arid and semi-arid regions of the world.

A significant proportion of arid and semi-arid areas of South America are located in Argentina (Fensholt et al., 2012). AGB and plant cover have been estimated at a regional scale based on remote sensing technologies in Argentinian dry forestlands (Gasparri et al., 2010; Gasparri and Baldi, 2013; González-Roglich and Swenson, 2016) and shrublands. However, the wide range of variations in climate, physiognomy, and floristic composition throughout the arid and semi-arid areas in Argentina makes it clear that many local and regional estimations are still necessary.

In this study, we estimated AGB in semi-arid woody vegetation in Northeast Patagonia, Argentina. We evaluated whether AGB at the stand level can be estimated from plant cover and to what extent the estimation accuracy is improved by the inclusion of other field-measured structure variables. We also evaluated whether the relationship between field-measured plant cover and remote sensing estimates can be used to reliably estimate and map the regional biomass.

2 Methods and materials

2.1 Study area

The study area is located in Northwest Patagonia, Argentina, which is in the transition between the Espinal and Monte Ecoregions, within the geographical coordinates of 38°00′–41°00′S and 64°28′–62°15′W (Morello et al., 2012; Oyarzabal et al., 2018) (Fig. 1). The zonal vegetation is the shrub-steppe with the height of 1.5–3.0 m and vegetation cover of 50.0%–80.0%. The most common shrub species are *Larrea divaricata* Cav., *Chuquiraga erinacea* D. Don subsp. *erinacea*, *Condalia microphylla* Cav., *Monttea aphylla* (Miers) Benth. & Hook, *Prosopis flexuosa* DC. var. *depressa* F. A. Roig., and *Schinus johnstonii* F. A. Barkley (Roig et al., 2009; Torres Robles et al., 2015). Tree species are *Greoffroea decorticans* (Gillies ex Hook. & Arn.) Burkart (3.0–6.0 m in height), *Prosopis caldenia* Burkart (>6.0 m in height), and *Prosopis flexuosa* DC. var. *flexuosa* Phil. (>6.0 m in height). These tree species are found as sparse trees or in small groups (<1 hm^2) (León et al., 1998; Morello et al., 2012; Torres Robles et al., 2015).

The climate is sub-temperate transitional dry, with warm summers and moderately cold winters, and windy, especially in spring and summer. Precipitation varies in a Southwest–northeast gradient, approximately from 300 to 590 mm/a, with maximums in autumn and spring and high variability between years (Godagnone and Bran, 2009). Winters usually alternate between water surplus and water deficit (Gabella and Campo, 2016). Besides, soil water deficit exhibits in every spring, summer, and the beginning of autumn (October to April or May), with the maximum soil water stress occurring in the middle of summer (January) (Gabella and Campo, 2016).

2.2 Experimental design

Mean AGB of woody vegetation was estimated using a model-based ratio estimator (Kangas and Maltamo, 2006). First, we sampled the woody vegetation structure in 42 sampling sites (see Fig. 1) between 2010 and 2012. Second, we estimated the biomass by direct harvest in 21 out of the 42 sites between 2014 and 2016. Third, we fitted a model to estimate the AGB of the 42 sampling sites using stand-level plant cover as the independent variable. We fitted a second model using the AGB of the 42 sampling sites as the dependent variable and LANDSAT TM bands as independent variables. Finally, we estimated AGB at the regional scale and calculated the ratio between stand structure-based and satellite-based biomass estimates. From this ratio, we estimated the mean biomass for the whole study area and calculated its sampling error.

2.3 Stand structure field sampling

Stand structure was assessed in 42 sampling sites selected from the visual analysis of very high-resolution images on the Google Earth platform. Based on such analysis, we selected the sampling sites that represent a gradient of vegetation cover between low and high, according to Di Gregorio and Jansen (2000) to achieve appropriate spatial distribution. Due to this non-random

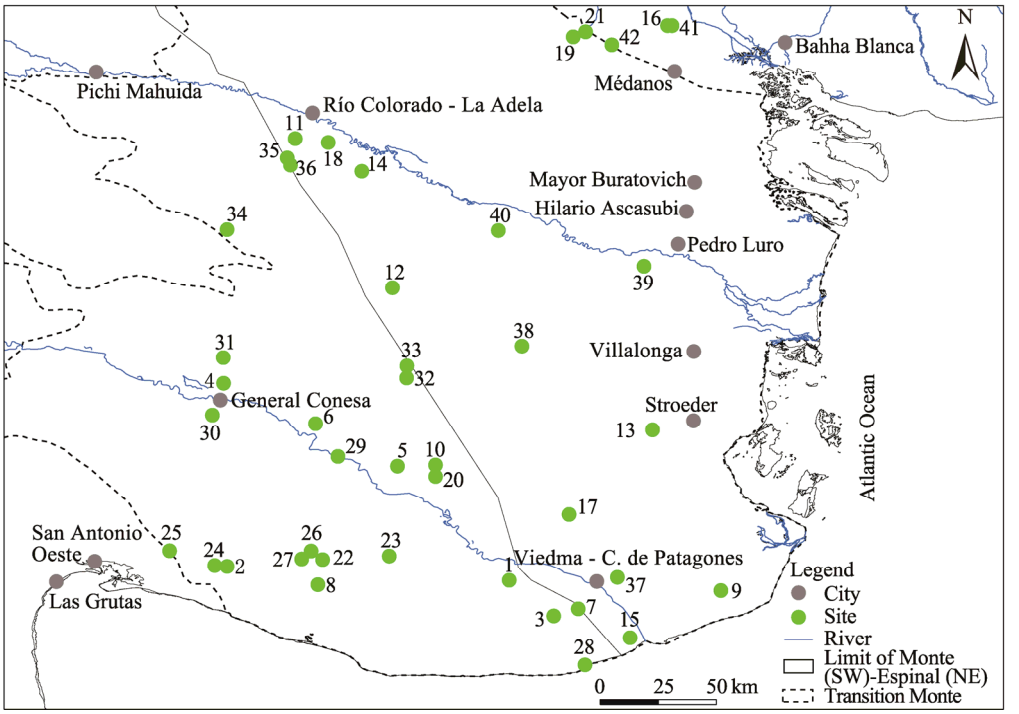

Fig. 1 Geographical location of the study area and distribution of sampling sites. Structural survey sites: 1–42; harvest sites for biomass estimation: 1–21. The solid line indicates the limit between "Monte" (southwest) and "Espinal" (northeast) ecoregions according to Morello et al. (2012), and the dotted line indicates the boundary of the transitional vegetation unit "Transition Monte", according to Oyarzabal et al. (2018).

sampling procedure, we used model-based estimation (Kangas and Maltamo, 2006). In each site, the sample unit consisted of three 10 m×10 m plots which were established along a transect line with a distance of 70 m between plots. We located the starting point of the transect and selected its direction, so that the sample unit matched the selected plant cover category that were detected in the Google Earth images. We considered three woody plant categories: (1) large individuals, referring to single-stemmed plants separated from other plants(at least 5 cm in diameter at the stem base); (2) small individuals, referring to multi-stemmed plants separated from other plants or single-stemmed plants with DBH<5cm (stem diameter at 1.3 m in height); and (3) plant groups, including two or more small individuals, with the same or different species, and crowns in contact. We recorded the following measurements: (1) total height, as the distance between the highest point of the plant crown and the soil; (2) DBH, as the diameter of the stem at 1.3 m in height, only for large individuals; and (3) crown diameters, as the maximum diameter of the crown of individuals or groups, and a second measurement of a perpendicular diameter. Plant height was measured with an optical clinometer or a metric stick for plants less than 2.0 m in height. DBH was measured with a diametric tape and crown diameters with a metric tape. Based on these measurements, we calculated total plant cover (coverT) at the plot level as the sum of the crown cover of individuals and groups of plants divided by the plot area. The crown cover for each plant was approximated to the area of a circle of diameter equal to the average of maximum and perpendicular diameters. We calculated the maximum and average heights of the plot based on the height of individuals and plant groups. Basal area was calculated for every individual with DBH greater than 5 cm.

2.4 Local-scale AGB estimation

Based on the structure sampling, we selected 21 sites for biomass estimation. The selected sites approximately represented the observed range of woody vegetation cover, as well as even spatial distribution. In each of the 21 sites, a 5 m×5 m plot was centered in the third plot where stand

structure was previously sampled. In this plot, plant cover, height, and DBH were measured as described previously and all the above-ground parts of the woody plants were harvested. Plant parts were weighted in the field in separate categories: (1) leaves and branches with diameter less than 1 cm; (2) stems or branches with diameter of 1–5 cm; (3) stems or branches with diameter of 5–10 cm; and (4) stems with diameter greater than 10 cm. Aliquots of different categories were collected and oven-dried to constant weight to determine the humidity factors. We then estimated the dry biomass for each harvested plot, based on the field weights and the humidity factors.

We fitted a linear model to estimate AGB from plant cover in the plot and evaluated whether the model fit improved with the inclusion of basal area, maximum height, average height, or the cover of different plant categories (plants with DBH of less than 5 cm, in the range of 5–10 cm, and greater than 10 cm). We selected the final model was selected based on the Akaike Information Criterion (AIC), which is an appropriate measure to compare models with a different number of independent variables (Burnham and Anderson, 2002). The P values of the slope of independent variables and coefficient of determination (R^2) were also indicated. Plots of fitted vs. observed values, as well as the histograms of the residuals, were used to visually evaluate the adequacy of the selected model and variables transformation (natural logarithm). The fitted linear model was applied to estimate AGB in all 42 sites where the woody vegetation structure was measured. Data were analyzed by Infostat software (di Rienzo et al., 2016).

2.5 Regional-scale AGB estimation and mapping

The biomass estimated for the 42 sites based on the stand structure was used to fit a linear model at a regional scale, using the LANDSAT 5 TM bands as independent variables (path 227–228 and row 088–087–086). The images were obtained from United States Geological Survey (www.usgs.gov). The fit of models to estimate plant biomass based on LANDSAT bands and vegetation indices can strongly vary among dates due to variations in plant and soil absorption and reflection responses (Gasparri et al., 2010). Thus, we analyzed images free of clouds between 2007 and 2011 to cover different phenological phases and seasons, with are close to the dates of vegetation sampling. By visual interpretation, we ensured that no sample site was affected by land-use change within the time range of the LANDSAT image dates. A geometric and radiometric correction was applied to all images to remove data acquisition errors (González-Iturbe Ahumada, 2004). The Rayleigh correction was applied to all images to calculate the reflectance at the surface level (Kaufman, 1989). The following vegetation indices were also calculated: Normalized Difference Vegetation Index (NDVI) (Rouse et al., 1974), Enhanced Vegetation Index (EVI) (Huete et al., 2002), and Soil-Adjusted Vegetation Index (SAVI) (Huete, 1988). The mean of three pixels, corresponding to the location of each structure plot per site, was calculated for bands 1 to 7 (except the thermal infrared band 6), as well as for each vegetation index.

We fitted linear regression models for each image date. Since similar models used for estimating biomass only include one or two independent variables (Gasparri et al., 2010), we first explored the simple linear correlations between structure-based estimations of biomass and the following predictors: satellite bands and vegetation indices. The best-correlated variable was then included in the model, and the remaining variables were added one at a time. We used AIC to compare the fit of different models. Student t values were used to evaluate the significance of each variable in the model and the predicted vs. observed plots to visually explore the linearity and homoscedasticity of the residuals. Based on such plots, we determined whether log-linear transformations (natural logarithm) should be applied or not. R^2 was also indicated for each model. The selected model was applied to each pixel of the image with woody vegetation, for the corresponding date. We applied a map mask to exclude the AGB mapping for urban and agricultural areas as well as dunes, water bodies, and rocky areas. The mask was defined by using local maps.

2.6 Mean biomass estimation and sampling error

The mean biomass of the study area was calculated from the ratio between the mean structure-based biomass estimate (variable y) and the mean satellite-based biomass estimate (variable x) for 42 sampling sites. This ratio was multiplied by the mean satellite-based biomass estimation for the

entire images. Since the 42 sampling sites were selected to represent the observed range of woody plant cover, rather than following a sampling design, we estimated the sampling error for the model-based ratio estimation (Kangas and Maltamo, 2006). A bootstrap procedure was applied to estimate the sampling error (Gregoire and Salas, 2009; Mageto and Motubwa, 2018). This procedure consisted of four steps, as follows: (1) 21 pairs of values x (plant cover) and y (field-measured biomass) were randomly taken from 21 observed data with reposition; (2) the linear model was fitted to estimate biomass based on plant cover; (3) the biomass was estimated for 42 pairs of values randomly taken from the 42 sampling sites with repetition; and (4) the linear model was fitted to estimate biomass based on satellite variables (those selected in previous procedures), and the mean biomass was calculated by ratio estimation. This procedure was repeated 1000 times and the percentiles 5 and 95 were taken as 95% confidence limits. Additionally, we plotted the observed values (structure-based estimation of biomass) vs. predicted values (satellite-based estimations of biomass) obtained from all 1000 simulations. Percentile lines 5% and 95% were drawn using quantile regression for descriptive purposes.

3 Results

3.1 Vegetation structure data and local-scale AGB estimation

Total plant cover ranged between 18.7% and 95.2% in the 42 sites sampled for the estimation of vegetation structure (Table S1). The cover of plants with DBH less than 5 cm accounted for more than 80.0% of the total cover in 32 out of 42 sites, while the cover of plants with DBH greater than 5 cm accounted for a maximum of 40.0%–60.0% in only 5 of these 42 sites (Table S1; Fig. 2). Among the sampling sites where direct harvest was carried out, the cover of plants with DBH greater than 5 cm accounted for more than 50.0% of the total cover in 7 out of 21 sites (Table S2). Plant biomass mostly ranged between 2.0 and 70.8 Mg/hm^2 and reached a maximum of 161.1 Mg/hm^2 (Table S2).

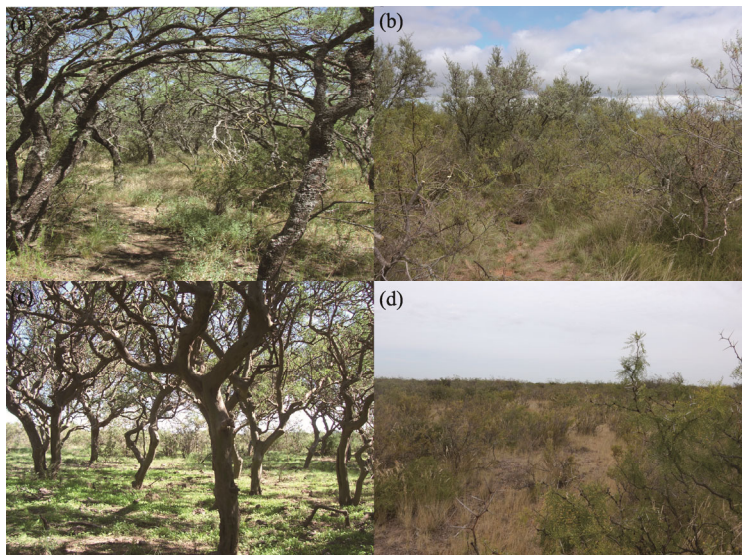

Fig. 2 Woody vegetation with different total coverages in the study region. (a), site 19 (cover of 95.2%); (b), site 12 (cover of 68.6%); (c), site 17 (cover of 71.4%); (d), site 2 (cover of 26.0%).

All the models used for estimating AGB based on structure variables fitted well (R^2>0.70 in all cases). The best linear trends in the observed-predicted plots were obtained from models fitted with log-transformed dependent and independent variables. The model fitted using only total cover as predictor exhibited a lower AIC than those including more detailed structure variables (Table 1). This model exhibited clear linear trends and homogeneous dispersion in the observed-predicted plot (Fig. 3). The maximum observed biomass followed the linear trend of all data.

Table 1 Models used to estimate above-ground biomass (AGB) based on structure variables

Model	*n*	b_0	b_1	b_2	b_3	AIC	R^2
$logAGB=b_0+b_1logCoverT$#	21	-4.62^{***}	1.92^{***}		-	31.9	0.80^{***}
$logAGB=b_0+b_1logCoverT+b_2BA$	21	-4.03^{**}	1.75^{***}	0.16^{NS}	-	32.6	0.80^{***}
$logAGB=b_0+b_1logCoverT+b_2$Mean height	21	-4.26^{**}	1.75^{***}	0.33^{NS}	-	32.1	0.81^{***}
$logAGB=b_0+b_1logCoverT+b_2$Max height	21	-4.18^{**}	1.75^{***}	0.11^{NS}	-	33.1	0.80^{***}
$logAGB=b_0+b_1Cover_{>10}+b_2Cover_{5-10}+b_3Cover_{<5}$	21	1.26^{**}	0.03^{***}	0.04^{**}	0.02^{NS}	38.4	0.75^{**}

Note: AGB, above-ground biomass; CoverT, total plant cover; BA, basal area; Max height, maximum height in the plot; Mean height, mean height in the plot; $Cover_{>10}$, vegetation cover of individuals with a diameter at breast height (DBH) greater than 10 cm; $Cover_{5-10}$, vegetation cover of individuals with DBH between 5 and 10 cm; $Cover_{<5}$, vegetation cover of individuals or groups with DBH less than 5 cm; n, number of sites; b_0, b_1, b_2, and b_3, coefficients; AIC, Akaike Information Criterion; R^2, coefficient of determination; *** and **, significance levels of 0.0001 and 0.01, respectively; NS, non-significant; -, no data. # means the selected model in this study.

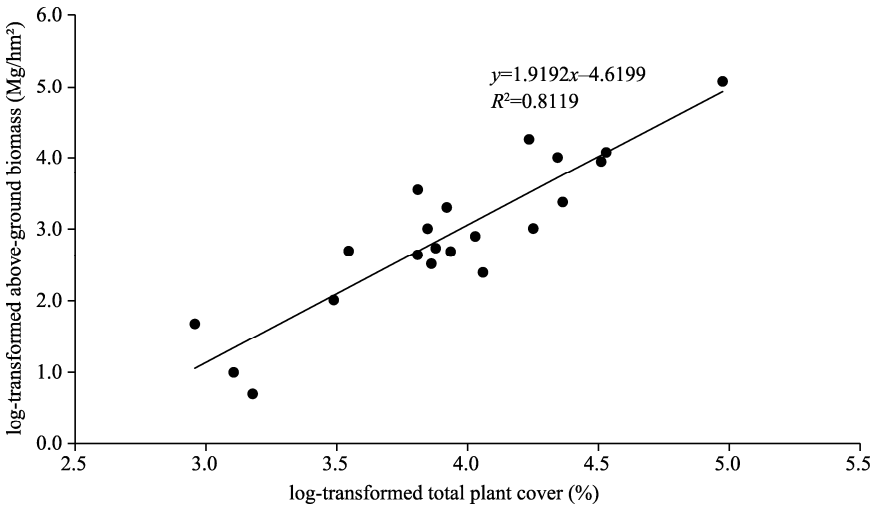

Fig. 3 Relationship between log-transformed total plant cover and log-transformed above-ground biomass. The selected model is plotted as a solid line.

3.2 Regional-scale AGB estimation from satellite data and mapping

High absolute correlations were found between AGB and individual bands as well as between AGB and vegetation indices. The greatest absolute correlations were observed in late spring and no significant correlations were observed in middle or late summer, as shown in Table 2. The best model to estimate log-transformed AGB was fitted with data from late spring, including the log-transformed band 3 as the first variable in the model. The log-transformed band 2 was retained as the second variable in the model, which exhibited an approximately linear trend between the observed and predicted values (Table 3; Fig. 4). No further variables were retained based on AIC values. The fitted AGB values ranged approximately between 2.5 and 70.3 Mg/hm^2.

Table 2 Pearson's correlation coefficient for the bands (LANDSAT TM) and green indices (NDVI, SAVI, and EVI) in relation to the biomass on different dates

Date (dd/mm/yy)	B1	B2	B3	B4	B5	B7	NDVI	SAVI	EVI
19/09/10	-0.41^{**}	-0.68^{***}	-0.61^{***}	-0.62^{***}	-0.66^{***}	-0.59^{***}	-0.06^{NS}	-0.29^{*}	-0.23^{NS}
10/10/10	-0.64^{***}	-0.68^{***}	-0.68^{***}	-0.75^{***}	-0.66^{***}	-0.58^{**}	0.05^{NS}	-0.33^{**}	-0.27^{*}
21/12/10	-0.63^{***}	-0.69^{***}	-0.76^{***}	-0.54^{**}	-0.69^{***}	-0.67^{***}	0.77^{***}	0.68^{***}	0.73^{***}
23/01/11	-0.32^{**}	-0.37^{**}	-0.39^{**}	-0.16^{NS}	-0.43^{**}	-0.39^{**}	0.41^{**}	0.28^{*}	0.31^{**}
17/03/07	-0.64^{***}	-0.68^{***}	-0.67^{***}	-0.17^{NS}	-0.62^{***}	-0.63^{***}	0.51^{**}	0.39^{**}	0.41^{**}

Note: B1, band 1; B2, band 2; B3, band 3; B4, band 4; B5, band 5; B7, band 7; NDVI, Normalized Difference Vegetation Index; SAVI, Soil-Adjusted Vegetation Index; EVI, Enhanced Vegetation Index; ***, **, and *, significance levels of 0.0001, 0.01, and 0.05, respectively; NS, non-significant.

Table 3 Regression models of AGB based on spectral data

Model	*n*	b_0	b_1	b_2	AIC	R^2
$logAGB=b_0+b_1logB2+b_2logB3$#	42	3.64^{NS}	11.77^{**}	-11.30^{***}	62.3	0.62^{***}
$AGB=b_0+b_1NDVI$	42	-31.23^{***}	226.48^{***}	-	75.1	0.58^{***}
$logAGB=b_0+b_1logB4$	42	-5.70^{***}	-4.34^{***}	-	93.1	0.56^{***}
$AGB=b_0+b_1EVI$	42	-34.12^{**}	304.37^{***}	-	76.7	0.52^{***}

Note: The B2, B3, NDVI, and EVI were dated on 21 December 2010. The B4 was dated on 10 October 2010. *** and **, significance levels of 0.0001 and 0.01, respectively; NS, non-significant; -, no data. # means the selected model in this study.

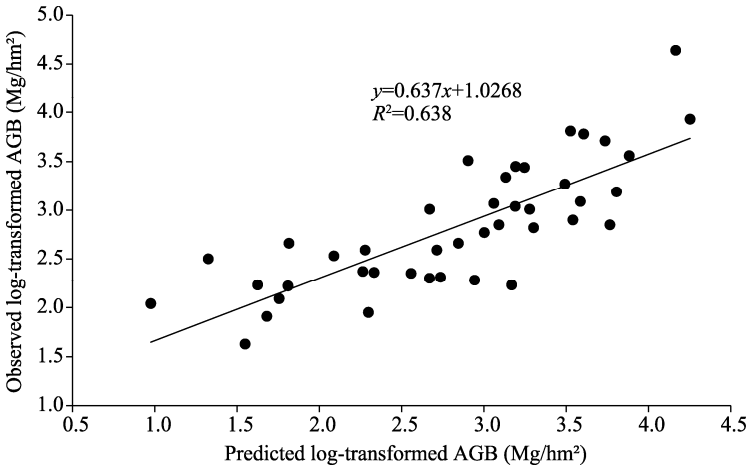

Fig. 4 Predicted vs. observed values of the regression of log-transformed AGB based on bands 2 and 3. The solid line indicates a linear model with intercept=0 and slope=1.

The application of the model to the entire study area yielded a predicted biomass ranging between 4.9 and 96.7 Mg/hm^2. A clear spatial trend was apparent on the map (Fig. 5). The highest AGB values of woody vegetation were found in the study area where rainfall is higher, while the lowest values were observed towards the southwestern part, where rainfall is lower. In this sense, at the regional level, AGB of woody vegetation decreased from northeast to southwest (Fig. 5a). However, high biomass values were observed along the entire gradient (Fig. 5b). Regarding the biomass categories, 58.0% of the surface land had values between 5.0 and 10.0 Mg/hm^2, and 32.0% showed values between 10.0 and 20.0 Mg/hm^2, that is, 90.0% of the region yielded AGB values between 5.0 and 20.0 Mg/hm^2 (Fig. 5a). In contrast, 10.0% of the region exhibited AGB ranging from 20.0 Mg/hm^2 to more than 60.0 Mg/hm^2.

The mean AGB in study area was 11.9 Mg/hm^2 by ratio estimation (8.0–16.0 Mg/hm^2) (Fig. 6). The total AGB of the study area (0.60×10^6 km^2) was 72.4 Tg, equivalent to a carbon stock of 36.2 Tg C. The bootstrap-based confidence interval yielded a sampling error of about 33.0%. The bootstrapped predicted-observed plot showed an approximately linear trend while the effect of influencing local data was observed for predicted biomass of about 25.0 Mg/hm^2. The lines of 5.0% and 95.0% quantile regression showed symmetric departures from the expected predicted-observed relationship (intercept=0, slope=1).

4 Discussion

4.1 Local-scale AGB estimation

Total plant cover allowed us to obtain accurate estimates of AGB. There were wide differences between sites in the cover of different plant size categories as well as in the mean height and maximum height. Despite the structure variation, the estimate of AGB based on the total cover was not improved by including more structure variables in the model. The cover of the smaller plants (plants with DBH less than 5 cm or stem height below 1.3 m) was clearly the most important component of woody vegetation.

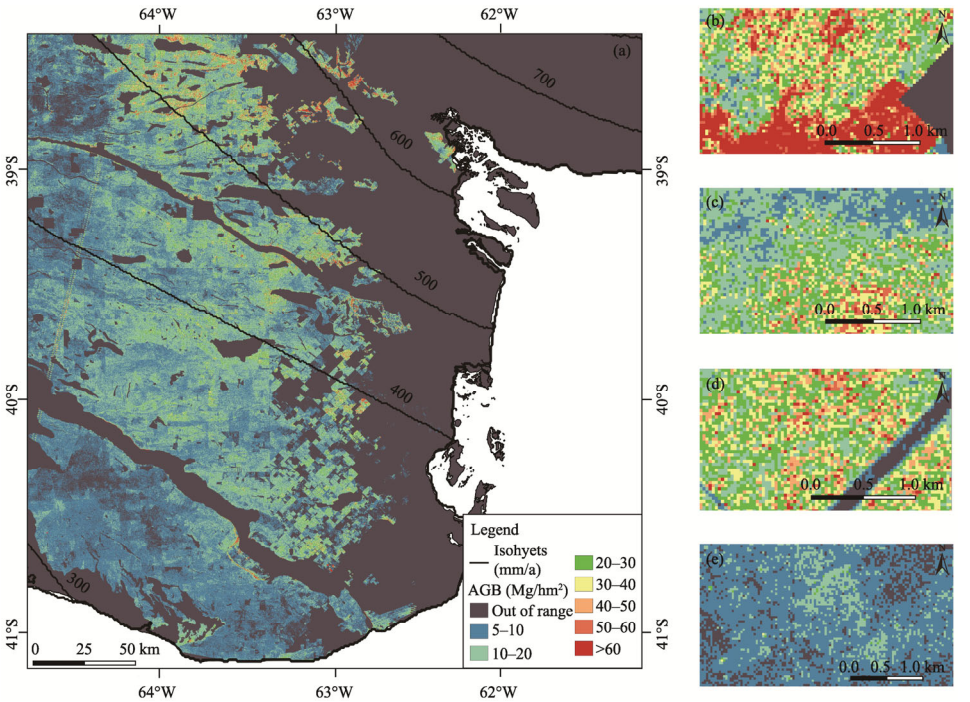

Fig. 5 AGB mapped for the entire study area based on LANDSAT TM bands 2 and 3 (a), and cut-offs of AGB along the geographic gradient (b–e). Isohyets reflects the mean annual precipitation.

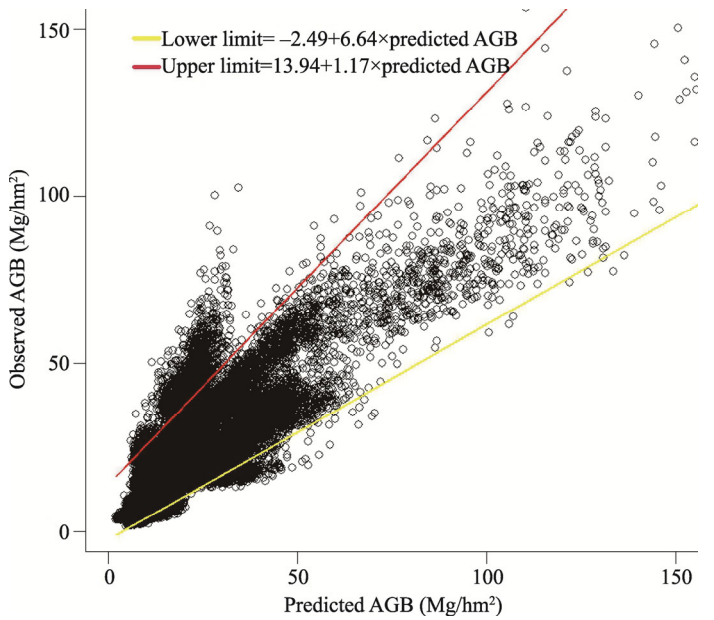

Fig. 6 Predicted vs. observed plots of the model of AGB based on bands 2 and 3 in 1000 permutations of the bootstrap procedure. Solid and discontinuous lines exhibit 95% upper and lower confidence limits (5 and 95 quantiles, respectively).

Stem diameter and plant height may be needed for the accurate estimation of biomass of woody vegetation (Chojnacky and Milton, 2008; Pearce et al., 2010); however, plant cover demonstrated to be a suitable predictor of biomass measured at the field scale or using remote sensing technologies (González–Roglich and Swenson, 2016; Pordel et al., 2018; Fusco et al., 2019). In Argentina, different studies have found that models to estimate the individual shrub weight based

only on crown cover or diameter and those including plant height had a similar fit. Oñatibia et al. (2010) found that in semi-arid, cold-temperate shrublands of central Patagonia, Argentina, the individual weight of three dominant shrub species was similarly estimated by models based on the average crown diameter and those models including total plant height. Similarly, in semi-arid, warm-temperate shrublands, the crown diameter was the best estimator of individual plant weight in shrub species while stem diameter was the best estimator of tree species (Hierro et al., 2000). All the species in that study are found in our study area. Finally, in semi-arid woody vegetation of northern Argentina (Chaco region), crown area was the best estimator of individual plant weight in single-variable models for eight shrub species with the height ranging between 1.0 and 4.0 m (Conti et al., 2013). Moreover, crown area was the best estimator of individual plant weight for all species-pooled data. These studies explain at the individual plant level what we found at the stand level.

Stand-level AGB estimates of semi-arid woody vegetation in Argentina are scarce given the wide distribution area and variable climate. The stand-level plant cover we estimated ranged between 18.7% and 95.2% and AGB between about 2.0 and 70.8 Mg/hm^2. These estimates are lower than those found for the stand-level subtropical Chaco forests in semi-arid regions (45.0–135.0 Mg/hm^2; Gasparri et al., 2010) and those found for the semi-arid warm-temperate Espinal savanna (about 5.0–100.0 Mg/hm^2; González–Roglich and Swenson, 2016). On the other hand, the stand-level AGB we estimated was higher than the AGB of warm-temperate Monte shrublands (7.0–8.0 Mg/hm^2; Zivkovic et al., 2013), above the semi-arid cool temperate Monte shrublands in east of Patagonia (about 10.0–30.0 Mg/ hm^2, Bertiller et al., 2004), and the cool temperate shrublands in northwest (10.0–14.0 Mg/hm^2, Nosetto et al., 2006) and south (5.0–20.0 Mg/hm^2; Peri, 2011) of Patagonia. Thus, the AGB we estimated follows a decreasing north–south gradient of semi-arid ecosystem, and large geographical gaps need to be filled.

4.2 Regional estimate of AGB and mapping

Total plant cover was well estimated from LANDSAT TM. Different results were reported regarding the estimation of plant cover or biomass based on satellite bands or indices. Many studies found that vegetation indices are good predictors of plant cover or biomass (Gasparri et al., 2010; Yan et al., 2013; Pordel et al., 2018; Fusco et al., 2019), while individual LANDSAT TM bands or linear combinations were also reported to be good predictors (Chen and Gillieson, 2009; Chen et al., 2018; Lopez Serrano et al., 2020). The estimation of vegetation variables based on remote sensing products is also dependent on seasonal vegetation changes (Chen and Gillieson, 2009; Gasparri et al., 2010; Issa et al., 2020). Here, we found the linear combination of LANDSAT TM bands 2 and 3 at the end of spring, to be the best predictor of field-measured plant cover. Typically, vigorous vegetation shows a reduced reflectance in blue and red wavelengths (visible bands 1 and 3, respectively) and a relative maximum reflectance in the green portion of the spectrum (band 2) (Navone, 2003). In this sense, the coefficients of bands 2 and 3 in the model were positive and negative, respectively, and the model fitted well right before the dry season begins.

The good fit of the model for estimating AGB based on LANDSAT bands allowed us to estimate a reliable ratio of regional biomass to woody vegetation. The use of ratio estimation is recommended if the Pearson linear correlation is above 0.60 between the target variable (the estimation of AGB based on total plant cover measured in the field) and the auxiliary variable (fitted values of the model based on LANDSAT bands 2 and 3) (Kangas and Maltamo, 2006). This condition is largely satisfied since the model fit is greater than 60.0% (R^2=0.63). The "model-based" condition of our ratio estimator of mean AGB is attributed to the fact that we did not follow a sampling design to select the sites in which target and auxiliary variables were simultaneously observed. Instead, these sites were selected to represent a gradient in plant cover in an approximately even spatial distribution throughout the study area. Due to this non-probabilistic selection of the sampling sites, the reliability of the estimation relies on the adequacy of the model and constitutes a recommended procedure for the estimation of mean AGB from remote sensing and its sampling error (Ståhl et al., 2016). Since the AGB was estimated based on field-measured

total plant cover, we used a bootstrap procedure, rather than the standard formulas given, for example, by Kangas and Maltamo (2006), to calculate the sampling error. The bootstrap was carried out by resampling the database that we used to fit the regression of AGB on plant cover, both measured in the field, as well as the regression of AGB estimated from plant cover on LANDSAT bands. Thus, the entire estimation procedure was taken into account in the estimation of the sampling error.

The mean model-based ratio estimate of AGB was clearly under the middle point of the field observed and of the estimated AGB because the pixels with low estimated AGB were far more frequent than the pixels with high estimated AGB. Mean and sampling error estimates over large areas are needed to quantify the contribution of woody vegetation to the ecosystem carbon stock. The mean AGB found (approximately 12.0 Mg/hm^2) represented a mean carbon stock of approximately 6.0 Mg/hm^2, which was slightly lower than the carbon stock reported for the Espinal savannas (8.0 Mg/hm^2), located about 250 km to the northwest of the study area in more humid and warmer climate conditions. Sampling error (about 30.0%) and the estimation area size were also similar between both studies: 0.50×10^6 km^2 in González–Roglich and Swenson (2016) and 0.61×10^6 km^2 of woody vegetation in this study.

The geographical gradient of local AGB shown by satellite-based estimates clearly agrees with a climate gradient and the structural geographical variations described by Torres Robles et al. (2015). The mean annual precipitation ranges from 500–600 mm/a in north–northeast of the study area to 300–400 mm/a in south–southwest of the study area. The maximum local AGB in the map ranges from >60.0 Mg/hm^2 to about 5.0–10.0 Mg/hm^2 in the same geographical gradient. The maximum satellite-based estimates of AGB are similar to the satellite-based estimates of AGB in subtropical semi-arid Chaco forests (about 54.0 Mg/hm^2) reported by Gasparri and Baldi (2013) at the driest end of a precipitation gradient in northern Argentina (about 400 mm/a). This highlights the important role that the extensive semi-arid shrublands play in carbon storage.

Shoshany and Karnibad (2015) proposed a model to estimate the AGB in semi-arid shrublands in Israel. Based on this model, they estimated a maximum AGB of about 40.0 and 15.0 Mg/hm^2 for mean annual precipitation of 550 and 350 mm/a, respectively. These values are similar to those estimated in the present study if the uncertainty of such estimates is taken into account. Local AGB is greatly affected by land use (Shoshany and Karnibad, 2015), and Torres Robles et al. (2015) reached the same conclusion in relation to woody vegetation structure in the study area. A high small-scale spatial variation in AGB is observed in east-southeast of the study area, where intensive land-use change affects the woody vegetation structure (Torres Robles et al., 2015).

5 Conclusions

Total plant cover allowed us to obtain a reliable estimation of local AGB, and no better fit was attained by the inclusion of other structure variables. In turn, AGB calculated from total plant cover was well estimated from LANDSAT TM bands 2 and 3, which allowed us to obtain a model-based ratio estimate of the regional mean AGB and its sampling error. The biomass in the region ranged from 96.7 Mg/hm^2 in northeast to 4.9 Mg/hm^2 in southwest, with an average value for the region of 11.9 Mg/hm^2 (an error of 33.0%). The mean AGB of woody vegetation can greatly contribute to carbon storage in arid and semi-arid lands.

Knowing the mean AGB in the region provides us with a useful tool to estimate the impact of land-use change on the carbon balance of these ecosystems. In this context, our results show the importance of estimating AGB from woody cover and remote sensors, which should be used formally in woody vegetation biomass monitoring systems in arid and semi-arid ecosystems.

Acknowledgments

This research was funded by the National University of Río Negro Research Project (40-C-658) and the Research Project National Institute of Agricultural Technology, University Association of Higher Agricultural Education and National Council of Veterinary Deans (Proyect 940175). This work is part of Laura B RODRIGUEZ's Ph.D. thesis

supported by a scholarship from National Council of Scientific and Technical Research, Argentina. Special thanks to Dr. Timothy GREGOIRE, who kindly helped us to define the procedure for sampling error estimation.

References

Baccini A, Laporte N, Goetz S J, et al. 2008. A first map of tropical Africa's above-ground biomass derived from satellite imagery. Environmental Research Letters, 3(4): 045011, Doi: 10.1088/1748-9326/3/4/045011.

Bertiller M B, Bisigato A J, Carrera A L, et al. 2004. Structure of the vegetation and functioning of the ecosystems of Monte Chubutense. Bulletin of the Argentine Botanical Society, 39(3–4): 139–158. (in Spanish)

Burnham K P, Anderson D R. 2002. Model Selection and Multimodel Inference: A Practical Information–Theoretic Approach. New York, NY: Springer, 261–303.

Cartus O, Kellndorfer J, Walker W, et al. 2014. A national, detailed map of forest aboveground carbon stocks in Mexico. Remote Sensing, 6(6): 5559–5588.

Chave J, Andalo C, Brown S, et al. 2005. Tree allometry and improved estimation of carbon stocks and balance in tropical forests. Oecologia, 145(1): 87–99.

Chen W, Cao C X, He Q S, et al. 2010. Quantitative estimation of the shrub canopy LAI from atmosphere–corrected HJ–1 CCD data in Mu Us Sandland. Science China Earth Sciences, 53: 26–33.

Chen W, Zhao J, Cao C, et al. 2018. Shrub biomass estimation in semi-arid sandland ecosystem based on remote sensing technology. Global Ecology and Conservation, 16: e00479, doi: 10.1016/j.gecco.2018.e00479.

Chen Y, Gillieson D. 2009. Evaluation of Landsat TM vegetation indices for estimating vegetation cover on semi-arid rangelands: A case study from Australia. Canadian Journal of Remote Sensing, 35(5): 435–446.

Chojnacky D C, Milton M. 2008. Measuring carbon in shrubs. In: Hoover C M. Field measurements for forest carbón monitoring. New York: Springer, 45–72.

Conti G, Enrico L, Casanoves F, et al. 2013. Shrub biomass estimation in the semiarid Chaco forest: A contribution to the quantification of an underrated carbon stock. Annals of Forest Science, 70: 515–524.

Conti G, Gorné L D, Zeballos S R, et al. 2019. Developing allometric models to predict the individual aboveground biomass of shrubs worldwide. Global Ecology and Biogeography, 28(7): 961–975.

Dengsheng L. 2006. The potential and challenge of remote sensing−based biomass estimation, International Journal of Remote Sensing, 27 (7): 1297-1328

di Gregorio A, Jansen L J M. 2000. Land Cover Classification System (LCCS): classification concepts and user manual. FAO/UNEP/Cooperazione Italiana, Rome, 20–31.

di Rienzo J A, Casanoves F, Balzarini M G, et al. 2016. InfoStat Versión 2016. Grupo InfoStat, FCA, National University of Córdoba, Argentina. http://www.infostat.com.ar.

Dong J, Kaufmann R K, Myneni R B, et al. 2003. Remote sensing estimates of boreal and temperate forest woody biomass: carbon pools, sources, and sinks. Remote Sensing of Environment, 84(3): 393–410.

Eisfelder C, Kuenzer C, Dech S. 2012. Derivation of biomass information for semi-arid areas using remote-sensing data. International Journal of Remote Sensing, 33(9): 2937–2984.

Fensholt R, Langanke T, Rasmussen K, et al. 2012. Greenness in semi-arid areas across the globe 1981–2007—an Earth Observing Satellite based analysis of trends and drivers. Remote Sensing of Environment, 121: 144–158.

Flombaum P, Sala O E. 2007. Cover is a good predictor of aboveground biomass in arid systems. Journal of Arid Environments, 73(6): 597–598.

Foley J A, DeFries R, Asner G P, et al. 2005. Global consequences of land use. Science, 309(5734): 570–574.

Fonseca W G, Alice F G, Rey J M. 2009. Models to estimate the biomass of native species in plantations and secondary forests in the Caribbean zone of Costa Rica. Bosque, 30(1): 36–47. (in Spanish)

Fusco E J, Rau B M, Falkowski M, et al. 2019. Accounting for aboveground carbon storage in shrubland and woodland ecosystems in the Great Basin. Ecosphere, 10(8): e02821, doi: 10.1002/ecs2.2821.

Gabella J, Campo A M. 2016. Fragility and environmental degradation in rural areas of the temperate arid Argentinian diagonal. Estudios Geográficos, 77 (281): 491–519. (in Spanish)

Galidaki G, Zianis D, Gitas I, et al. 2017. Vegetation biomass estimation with remote sensing: focus on forest and other wooded land over the Mediterranean ecosystem. International Journal of Remote Sensing, 38(7): 1940–1966.

Gasparri N I, Parmuchi M G, Bono J, et al. 2010. Assessing multi–temporal Landsat 7 ETM+ images for estimating above–ground biomass in subtropical dry forests of Argentina. Journal Arid Environments, 74(10): 1262–1270.

Gasparri N I, Baldi G. 2013. Regional patterns and controls of biomass in semiarid woodlands: lessons from the Northern

Argentina Dry Chaco. Regional Environmental Change, 13(6): 1131–1144.

Gasparri N I, Grau H R, Gutierrez–Angonese J. 2013. Linkages between soybean and neotropical deforestation: Coupling and transient decoupling dynamics in a multi–decadal analysis. Global Environmental Change–Human and Policy Dimensions, 23(6): 1605–1614.

Godagnone R E, Bran D E. 2009. Integrated inventory of the natural resources of the province of Río Negro. Buenos Aires: INTA, 319–363. (in Spanish)

González–Iturbe Ahumada J A. 2004. Introduction to remote sensing: sampling techniques for natural resource managers. Mexico: Autonomous University of Mexico, Autonomous University of Yucatán National Council of Science and Technology, and National Institute of Ecology, 455–471. (in Spanish)

González–Roglich M, Swenson J. 2016. Tree cover and carbon mapping of Argentine savannas: Scaling from field to region. Remote Sensing of Environment, 172: 139–147.

Grainger A. 1999. Constraints on modelling the deforestation and degradation of tropical open woodlands. Global Ecology and Biogeography, 8: 179–190.

Gregoire T G, Salas C. 2009. Ratio estimation with measurement error in the auxiliary variate. Biometrics, 65(2): 590–598.

Grünzweig J M, Lin T, Rotenberg E, et al. 2003. Carbon sequestration in arid-land forest. Global Change Biology, 9(5): 791–799.

GTOS. 2010. A framework for terrestrial climate-related observations and development of standards for the terrestrial essential climate variables: proposed work plan. [2016-11-20]. http://www.fao.org/gtos/doc/pub78.pdf.

Hansen M C, Potapov P V, Moore R, et al. 2013. High-resolution global maps of 21st-century forest cover change. Science, 342(6160): 850–853.

Hengeveld G M, Didion M, Clerkx S, et al. 2015. The landscape-level effect of individual–owner adaptation to climate change in Dutch forests. Regional Environmental Change, 15: 1515–1529.

Hierro J L, Branch L C, Villarreal D, et al. 2000. Predictive equations for biomass and fuel characteristics of Argentine shrubs. Journal of Range Management, 53: 617–621.

Hofstad O. 2005. Review of biomass and volume functions for individual trees and shrubs in southeast Africa. Journal of Tropical Forest Science, 17(1): 151–162.

Houghton R A. 2005. Aboveground forest biomass and the global carbon balance. Global Change Biology, 11(6): 945–958.

Houghton R A. 2007. Balancing the global carbon budget. Annual Review of Earth and Planetary Sciences, 35: 313–347.

Huete A R. 1988. A soil–adjusted vegetation index (SAVI). Remote Sensing of Environment, 25: 295–309.

Huete A, Didan K, Miura T, et al. 2002. Overview of the radiometric and biophysical performance of the MODIS vegetation indices. Remote Sensing of Environment, 83(1–2): 195–213.

Issa S M, Dahy B S, Saleous N. 2020. Accurate mapping of date palms at different age-stages for the purpose of estimating their biomass. Annals of the Photogrammetry, Remote Sensing and Spatial Information Sciences, Volume 3. XXIVth International Society for Photogrammetry and Remote Sensing Congress. 4 July–10 July 2021. Nice, France, 461–467.

Jenkins J C, Chojnacky D C, Heath L S, et al. 2004. Comprehensive database of diameter–based biomass regressions for North American trees species. Delaware: US Department of Agriculture, Forest Service and Northeastern Research Station, 1–45.

Kangas A, Maltamo M. 2006. Forest Inventory: Methodology & Applications. Berlin: Springer, 357.

Kaufman Y J. 1989. The atmospheric effect on remote sensing and its correction. In: Asrar G. Theory and Application of Optical Remote Sensing. New York: Wiley Publication, 336–428.

Kindermann G, Obersteiner M, Sohngen B, et al. 2008. Global cost estimates of reducing carbon emissions through avoided deforestation. Proceedings of the National Academy of Sciences, 105(30): 10302–10307.

León R J C, Bran D, Collantes M, et al. 1998. Mean vegetation units of extra-Andean Patagonia. Austral Ecology, 8: 125–144. (in Spanish)

Le Polain de Waroux Y, Lambin E F. 2012. Monitoring degradation in arid and semi-arid forests and woodlands: the case of the argan woodlands (Morocco). Applied Geography, 32(2): 777–786.

Lopez Serrano P M, Cárdenas Domínguez J L, Corral–Rivas J J, et al. 2020. Modeling of aboveground biomass with landsat 8 oli and machine learning in temperate forests. Forests, 11(1): 11, https://doi: 10.3390/f11010011.

Mageto T, Motubwa J. 2018. Bootstrap confidence interval for model based sampling. American Journal of Theoretical and Applied Statistics, 7(4): 147–155.

Malagnoux M, Sène E H, Atzmon N. 2007. Forests, trees and water in arid lands: a delicate balance. Unasylva, 58: 24–29.

Morello J, Matteucci S D, Rodríguez A F, et al. 2012. Argentine ecoregions and ecosystem complexes. Buenos Aires: Graphic Orientation, 309–347. (in Spanish)

Navone S M. 2003. Remote Sensors Applied to the Study of Natural Resources. Buenos Aires: Faculty of Agronomy, University

of Buenos Aires, 81–95. (in Spanish)

Nosetto M D, Jobbágy E G, Paruelo J M. 2006. Carbon sequestration in semi-arid rangelands: Comparison of *Pinus ponderosa* plantations and grazing exclusion in NW Patagonia. Journal Arid Environments, 67(1): 142–156.

Oñatibia G R, Aguiar M R, Cipriotti P A, et al. 2010. Individual plant and population biomass of dominant shrubs in Patagonian grazed fields. Ecología Austral, 20: 269–279.

Oyarzabal M, Clavijo J, Oakley L, et al. 2018. Vegetation units of Argentina. Austral Ecology, 28: 040–063. (in Spanish)

Pearce H G, Anderson W R, Fogarty L G, et al. 2010. Linear mixed–effects models for estimating biomass and fuel loads in shrublands. Canadian Journal of Forest Research, 40(10): 2015–2026.

Peri P L. 2011. Carbon storage in cold temperate ecosystems in Southern Patagonia, Argentina. In: Islam Atazadeh. Biomass and Remote Sensing of Biomass. London, In Tech, 213–225.

Pordel F, Ebrahimi A, Azizi Z. 2018. Canopy cover or remotely sensed vegetation index, explanatory variables of above-ground biomass in an arid rangeland, Iran. Journal Arid Land, 10(5): 767–780.

Roig F A, Roig–Juñent S, Corbalán V. 2009. Biogeography of the Monte Desert. Journal of Arid Environments, 73(2): 164–172.

Rouse J W, Haas H R, Deering D W, et al. 1974. Monitoring the vernal advancement and retrogradation (green wave effect) of natural vegetation. NASA/GSFC Type III Final Report, Greenbelt, Md, 371.

Saatchi S S, Harris N L, Brown S, et al. 2011. Benchmark map of forest carbon stocks in tropical regions across three continents. Proceedings of the National Academy of Sciences, 108(24): 9899–9904.

Sankarán N M, Hanan N P, Scholes R J, et al. 2005. Determinants of woody cover in African savannas. Nature, 438(7069): 846–849.

Shoshany M, Karnibad L. 2015. Remote sensing of shrubland drying in the south–east Mediterranean, 1995–2010: Water–Use–Efficiency–Based mapping of biomass change. Remote Sensor, 7(3): 2283–2301.

Ståhl G, Saarela S, Schnell S, et al. 2016. Use of models in large–area forest surveys: comparing model–assisted, model–based and hybrid estimation. Forest Ecosystems, 3(5): 1–11.

Torres Robles S S, Arturi M, Contreras C, et al. 2015. Geographical variations of the structure and composition of the woody vegetation in the limit between the spinal and the mount in the Northeast of Patagonia (Argentina). Bulletin of the Argentine Botanical Society, 50 (2): 209–215. (in Spanish)

Yan F, Wu B, Wang Y. 2013. Estimating aboveground biomass in Mu Us Sandy Land using Landsat spectral derived vegetation indices over the past 30 years. Journal Arid Land, 5: 521–530.

Zeberio J M, Torres Robles S, Calabrese G M. 2018. Land use and conservation status of the woody vegetation of the Monte in the Northeast of Patagonia. Austral Ecology, 28: 543–552. (in Spanish)

Zeberio J M, Pérez C A. 2020. Rehabilitation of degraded areas in northeastern Patagonia, Argentina: Effects of environmental conditions and plant functional traits on performance of native woody species. Journal of Arid Land, 12: 653–665.

Zhang W, Brandt M, Wang Q, et al. 2019. From woody cover to woody canopies: How Sentinel–1 and Sentinel–2 data advance the mapping of woody plants in savannas. Remote Sensing of Environment, 234: 111465, doi: 10.1016/j.rse.2019.111465.

Zivkovic L, Martínez Carretero E, Dalmasso A, et al. 2013. Carbon accumulated in the plant biomass of the Villavicencio reserve (Mendoza – Argentina). Bulletin of the Argentine Botanical Society, 48(3–4): 543–551. (in Spanish)

Appendix

Table S1 Estimates of the structural variables for the analyzed sites

n	Mean height (m)	Maximum height (m)	$Cover_{>5}$ (%)	$Cover_{<5}$ (%)	CoverT (%)	BA (m^2)
3	0.78	1.50	0.0	18.7 (100.0)	18.7	
5	1.64	2.50	4.0 (18.0)	18.2 (82.0)	22.3	4.6
42	2.38	4.00	10.9 (46.0)	13.0 (54.0)	23.9	4.3
2	0.57	1.50	0.0	26.0 (100.0)	26.0	
9	1.28	2.00	0.0	26.7 (100.0)	26.7	
29	1.09	1.80	0.0	27.8 (100.0)	27.8	
41	1.56	2.00	0.0	28.5 (100.0)	28.6	
4	0.88	2.50	0.9 (3.0)	27.8 (97.0)	28.6	0.4
35	0.78	1.50	0.0	32.9 (100.0)	32.9	
8	0.77	1.50	0.0	36.0 (100.0)	36.0	
10	0.73	1.50	0.0	36.3 (100.0)	36.3	
22	1.11	1.70	0.0	36.6 (100.0)	36.6	
36	0.85	2.00	0.0	37.3 (100.0)	37.3	
34	0.91	2.00	0.0	41.8 (100.0)	41.8	
26	0.84	1.50	0.0	44.3 (100.0)	44.3	
6	1.03	2.00	0.0	44.3 (100.0)	44.3	
1	1.01	2.00	0.0	45.3 (100.0)	45.3	
31	1.03	4.00	19.8 (43.0)	26.0 (57.0)	45.8	2.2
11	1.07	1.50	0.0	48.3 (100.0)	48.3	
13	1.04	2.00	0.4 (1.0)	48.1 (99.0)	48.4	0.2
27	0.68	1.50	0.7 (1.0)	50.2 (99.0)	50.9	0.4
24	0.75	1.50	0.0	52.5 (100.0)	52.5	
32	1.01	2.00	0.0	54.1 (100.0)	54.1	
30	1.21	3.00	3.1 (6.0)	51.8 (94.0)	54.9	1.7
40	1.53	2.00	0.0	56.1 (100.0)	56.1	
23	1.13	2.10	0.0	57.1 (100.0)	57.1	
7	1.69	3.50	19.1 (33.0)	38.6 (67.0)	57.8	9.6
16	1.71	5.00	16.3 (28.0)	41.7 (72.0)	57.8	18.0
28	0.94	1.75	0.0	59.4 (100.0)	59.4	
15	1.25	2.00	0.0	60.4 (100.0)	60.4	
14	1.63	4.00	11.9 (19.0)	49.3 (81.0)	61.2	4.3
33	1.56	3.50	9.5 (14.0)	57.9 (86.0)	67.4	8.6
12	1.52	3.00	4.6 (7.0)	64.0 (93.0)	68.6	17.7
25	1.43	3.00	11.1 (16.0)	58.0 (84.0)	69.1	5.2
20	1.12	2.00	0.8 (1.0)	69.9 (99.0)	70.7	0.4
17	1.71	4.00	26.2 (37.0)	45.2 (63.0)	71.4	11.2
38	1.12	3.00	4.7 (6.0)	71.6 (94.0)	76.3	2.5
39	1.94	4.00	37.1 (48.0)	40.4 (52.0)	77.5	20.5
37	1.82	3.00	28.6 (36.0)	50.5 (64.0)	79.1	111.2
18	1.49	2.50	17.4 (21.0)	64.9 (79.0)	82.3	1.0
21	2.08	5.00	40.6 (44.0)	52.5 (56.0)	93.0	7.3
19	1.91	4.50	50.6 (53.0)	44.6 (47.0)	95.2	24.6

Note: *n*, number of sites; Mean height, mean height in the plot; Maximum height, maximum height in the plot; $Cover_{>5}$, vegetation cover of individuals with a diameter at breast height (DBH) greater than 5 cm. The percentage with respect to the total coverage is indicated in parentheses. $Cover_{<5}$, vegetation cover of individuals with a diameter at breast height (DBH) less than 5 cm. The percentage with respect to the total coverage is indicated in parentheses. CoverT, total plant cover; BA, basal area.

Table S2 Structural variables in the Monte-Espinal transition of NE Patagonia

n	CoverT (%)	Mean height (m)	Maximum height (m)	BA (m^2)	$Cover_{>10}$ (%)	$Cover_{5–10}$ (%)	$Cover_{<5}$ (%)	AGB (Mg/hm^2)
1	19.2	0.5	1.2	0.0	0.0	0.0	19.2	5.3
2	22.3	0.5	0.7	0.0	0.0	0.0	22.3	2.7
3	24.0	1.1	1.4	0.0	0.0	2.8	21.2	2.0
4	32.7	0.8	1.8	0.0	0.0	0.0	32.7	7.5
5	34.6	1.1	1.1	0.0	0.0	23.6	11.1	14.8
6	45.1	1.1	1.7	0.0	0.0	16.6	28.5	14.0
7	45.1	2.5	3.5	0.9	31.6	13.6	0.0	34.7
8	46.8	1.3	1.7	0.0	0.0	46.8	0.0	20.2
9	47.5	0.7	2.5	0.0	0.0	0.0	47.5	12.4
10	48.3	1.2	2.5	0.0	0.0	12.0	36.3	15.4
11	50.4	1.5	1.4	0.5	18.1	21.7	10.6	27.1
12	51.2	1.2	1.7	0.0	0.0	12.2	39.0	14.7
13	56.2	1.8	1.5	0.0	0.0	43.0	13.2	18.2
14	57.9	1.0	1.1	0.0	46.4	0.0	11.5	10.9
15	69.0	1.5	2.2	0.3	63.6	0.0	5.4	70.8
16	70.7	1.8	4.0	1.1	50.0	0.0	20.7	20.3
17	77.0	2.0	4.3	1.3	48.3	14.8	13.9	54.8
18	78.5	1.4	2.5	0.0	78.5	0.0	0.0	29.3
19	91.0	2.2	3.5	0.9	62.5	0.0	28.4	51.7
20	92.7	1.2	1.7	0.0	44.2	47.8	0.8	58.9
21	144.7	1.4	5.0	7.4	128.0	0.0	16.7	161.1

Note: *n*, number of sites; Cover T, total plant cover; Mean height, mean height in the plot; Maximum height, maximum height in the plot; BA, basal area; $Cover_{>10}$, vegetation cover of individuals with a diameter at breast height (DBH) greater than 10 cm; $Cover_{5–10}$, vegetation cover of individuals with DBH between 5 and 10 cm; $Cover_{<5}$, vegetation cover of individuals or groups with DBH less than 5 cm; AGB, above-ground biomass.